Neutralization–reionization study of the allyloxide anion

Detlef Schröder [a,*], Helmut Schwarz [b], Jana Roithová [c,*]

[a] Institute of Organic Chemistry and Biochemistry, Academy of Sciences of the Czech Republic, Flemingovo nám. 2, 16610 Prague 6, Czech Republic
[b] Institut für Chemie der Technischen Universität Berlin, Straße des 17. Juni 135, 10623 Berlin, Germany
[c] Department of Organic Chemistry, Faculty of Sciences, Charles University in Prague, Hlavova 8, 12083 Prague 2, Czech Republic

ARTICLE INFO

ABSTRACT
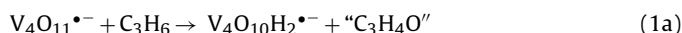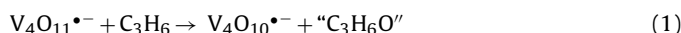
The charge-reversal (CR) and neutralization–reionization (NR) mass spectra of the mass-selected allyloxide anion $CH_2=CHCH_2O^-$ are reported. Similar to other alkoxide ions, the allyloxide anion shows only small abundances of the survivor cation in the CR and NR spectra. In combination with theoretical studies, the differences between the CR and NR experiments allow to explain why loss of atomic hydrogen corresponds to the major unimolecular decomposition channel of the neutral allyloxy radical. In addition, indirect evidence for an intramolecular rearrangement of the allyloxy radical to a carbon-centered oxiranyl methyl radical is provided. Interestingly, the patterns of the $C_3H_nO^+$ ions in the NR spectra show similarities to those of a recently reported photoionization study of oxygenated products formed upon interaction of $V_4O_{11}^{\bullet-}$ ions with propene. By extrapolation of our findings, we suggest that the reactions of the vanadium-oxide cluster anion $V_4O_{11}^{\bullet-}$ are initiated by allylic C–H bond activation of propene followed by oxygenation of the hydrocarbon fragment.

1. Introduction

While reactions of ions as well as neutral radicals with closed-shell neutral molecules have been subject of intense research in the last decades, experimental investigations of bimolecular reactions of two different open-shell species are much more scarce [1,2], if the stable NO_x radicals are excluded. Only recently have more radical/radical reactions became exploitable due to advances in experimentation [3,4]; for reviews on experimental and theoretical studies of radical-ion/radical reactions, we refer the reader to Refs. [5–7]. In this context, particular attention has been paid to the reaction of the allyl radical $C_3H_5^{\bullet}$ with atomic oxygen O (^3P) [8–14]. An obvious intermediate in this reaction is the allyloxy radical, $CH_2=CHCH_2O^{\bullet}$, which has also been extensively studied in the condensed phase [15–18] as well as in the gas phase [19]. The actual inspiration of the present work comes from a recent study of Siebert et al. [20], who investigated the neutral oxygenates formed upon interaction of the vanadium-oxide cluster radical anion $V_4O_{11}^{\bullet-}$ with propene in a dedicated experimental set-up in which the neutral products formed in the ion/molecule reaction are ionized by a pulse of a femtosecond laser operating in the ultraviolet (UV)

range. The ion chemistry observed inter alia suggests the occurrence of reaction (1), corresponding to an oxygen-atom transfer from the metal-oxide cluster to the hydrocarbon substrate; as a side-reaction H_2-uptake by the vanadium-oxide cluster [21,22] concomitant with the liberation of C_3H_4O has been observed (reaction (1a)).

$$V_4O_{11}^{\bullet-} + C_3H_6 \rightarrow V_4O_{10}^{\bullet-} + \text{"}C_3H_6O\text{"} \tag{1}$$

$$V_4O_{11}^{\bullet-} + C_3H_6 \rightarrow V_4O_{10}H_2^{\bullet-} + \text{"}C_3H_4O\text{"} \tag{1a}$$

In a conventional mass spectrometric set-up, however, only the mass differences of the ionic species (e.g., $\Delta m = -16$ for $V_4O_{11}^{\bullet-}$ and $V_4O_{10}^{\bullet-}$) are observed, while the nature of the neutral product remains unknown; for examples of the detection of the neutral products of metal-mediated reactions via mass spectrometric methods, see Refs. [23–26]. Plausible structures of a possible "C_3H_6O" product formed via oxygenation of propene are propene oxide (epoxidation), allyl alcohol (allylic oxidation), acetone and its enol form (both via O-atom attack at the central carbon atom followed by hydrogen migration), as well as propanal and its enol form (via attack of C(1) followed by keto-enol tautomerization). Siebert and coworkers managed to photoionize the neutral species formed in reaction (1) using a UV laser and the pattern observed in the mass range between 52 and 58 amu is reproduced in Fig. 1a. Compared to numerous neutralization–reionization (NR [27–30]) studies of other C_3H_6O species, the absence of a survivor ion at m/z 58, conjec-

* Corresponding author. Tel.: +420 220 183 463; fax: +420 220 183 462.
E-mail addresses: detlef.schroeder@uochb.cas.cz (D. Schröder), roithova@natur.cuni.cz (J. Roithová).
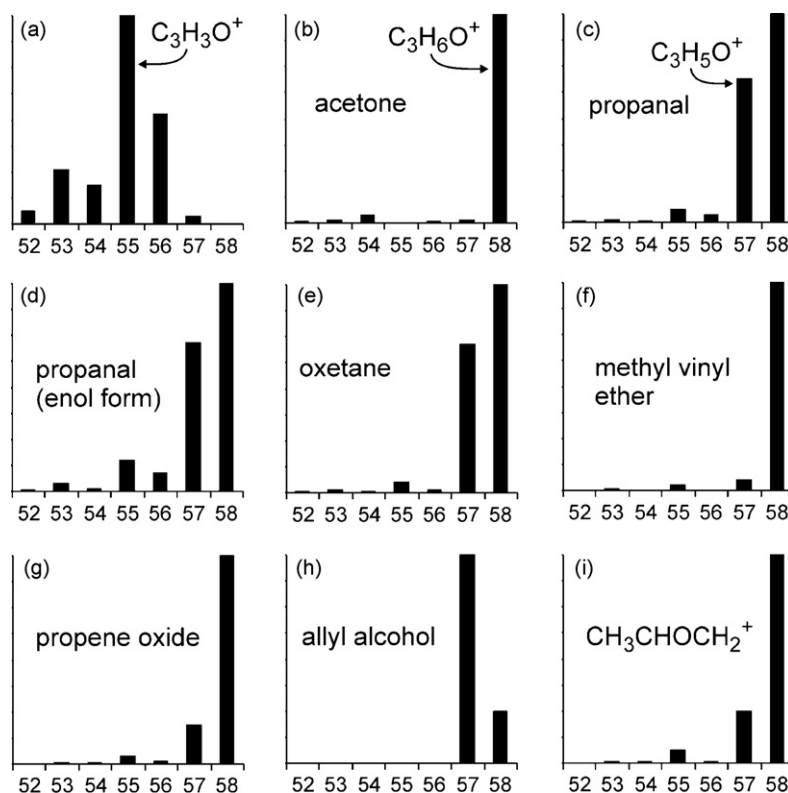
Fig. 1. Partial mass spectra of various C_3H_6O species in the region of the $C_3H_nO^+$ ions ($n = 0$–6, m/z 52–58). (a) Photo-ionized oxygenate from reaction (1) [20], (b) NR spectrum of $C_3H_6O^+$ from acetone (adopted from Fig. 4c of Ref. [27]), (c) NR spectrum of $C_3H_6O^+$ from propanal (adopted from Fig. 8c of Ref. [38]), (d) NR spectrum of $C_3H_6O^+$ from the enol form of propanal (adopted from Fig. 8a of Ref. [38]), (e) NR spectrum of $C_3H_6O^+$ from oxetane (adopted from Fig. 3c of Ref. [39]), (f) NR spectrum of $C_3H_6O^+$ from methyl vinyl ether (adopted from Fig. 4a of Ref. [39]), (g) NR spectrum of $C_3H_6O^+$ from propene oxide (adopted from Fig. 4c of Ref. [39]), and (h) NR spectrum of $C_3H_6O^+$ from allyl alcohol (made by reference to the partial spectrum given in Table 2 of Ref. [38]). (i) NR of the distonic ion $CH_3CHOCH_2^+$ (adopted from Fig. 4b of Ref. [39]). For additional data on the neutralization of $C_3H_6O^+$ ions, see [40,41].

tured for the neutral species generated in reaction (1), is somewhat surprising, however. In this respect, we refer to Fig. 1b–i, which show the mass regions of the survivor ions in NR spectra of several $C_3H_6O^+$ ions reproduced from previous studies. Upon reionization to cations, all these precursors are characterized by pronounced survivor ions at m/z 58 and/or an abundant fragment at m/z 57 (e.g., CH_2=$CHCHOH^+$ or $C_2H_5CO^+$). In marked contrast, photoionization of the oxygenate from reaction (1) does not yield any detectable m/z 58 and also the signal at m/z 57 is weak, while the largest peaks correspond to the hydrogen-depleted ions $C_3H_3O^+$ and $C_3H_4O^{\bullet+}$, m/z 55 and 56, respectively. While it would well be feasible to invoke other C_3H_6O isomers or to ascribe the differences to the very specific circumstances of the laser experiment of Siebert and coworkers, yet another option is that no genuine C_3H_6O but other C_3H_nO species with $n < 6$ are sampled in the photoionization experiment, for which the occurrence of reaction (1a) as a minor pathway is a direct indication. Given the facile allylic C–H bond activation of propene by gaseous metal-oxo species [31–33], we considered the involvement of the allyloxy radical $C_3H_5O^\bullet$, for which extensive fragmentation upon reionization to cations is expected to occur by analogy to the behavior of the corresponding saturated alkoxy radicals [34–37].

2. Experimental and computational methods

The experiments were performed using a modified VG ZAB/HF/AMD 604 four sector mass spectrometer of BEBE configuration (B stands for magnetic and E for electric sector) [42]. The $C_3H_5O^-$ ions were formed by chemical ionization (CI) of allyl alcohol using N_2O as a reagent gas in the negative ion

mode. CI was performed with electrons having a kinetic energy of 100 eV at a repeller voltage of about 0 V. Due to the excess of N_2O, the formation of allyloxide anions from the corresponding alcohol is likely to proceed via the reaction $N_2O + e^- \rightarrow N_2 + O^{\bullet-}$ as a first step, followed by deprotonation of the alcohol, i.e., $C_3H_5OH + O^{\bullet-} \rightarrow C_3H_5O^- + HO^\bullet$. After acceleration to 8 keV kinetic energy, the anions were mass-selected with B(1)/E(1). Charge reversal of the anions to cations was achieved in collision with molecular oxygen at 80% transmission (T) of the precursor ion beam. In the neutralization–reionization experiments, neutralization and reionization were achieved in two spatially separated collision cells (both O_2, 80%T) with a deflector electrode in-between which safely prevents any charged particles to enter the reionization volume. For a classification of the charge reversal (CR [43–46]) and neutralization–reionization experiments, we follow the terminology suggested by McMahon et al. [47] to distinguish the different variants of these electron-transfer experiments; $^-NR^+$, for example, refers to a neutralization–reionization process of an anion via the neutral species followed by reionization to cations. Further, the $^-NR^+$ and $^-CR^+$ spectra were analyzed with the NIDD method (neutral- and ion-decomposition difference) [48,49]. A $^-NIDD^+$ spectrum is obtained by subtracting a normalized $^-CR^+$ spectrum from the normalized $^-NR^+$ spectrum according to $I_{i,NIDD} = I_{i,NR}/\Sigma_i I_{i,NR} - I_{i,CR}/\Sigma_i I_{i,CR}$. The NIDD spectra thus include positive and negative signals. The positive signals can be traced back to preferential rearrangements or fragmentations occurring at the neutral stage and the negative signals to those that can be derived from ionic states. However, due to the different conditions that prevail in NR and CR experiments (e.g., a NR experiment per se requires two collision events whereas a CR experiment needs only

one), some particular features have to be pointed out: (i) the NR signals are generally broader compared to the CR spectra, (ii) fragmentation is often more extensive in NR than in CR, (iii) a slight shift of the apparent mass is observed between both spectra due to the kinetic energy lost in the collisionally driven electron-transfer processes, (iv) only NIDD intensities higher than |0.02| are assumed to be significant [48], and (v) only peak heights at unit mass resolution are considered, such that the NIDD spectra are usually presented as bar diagrams. Instead, here, we show the complete NIDD spectra which provide a more complete coverage of the experimental data and also account for differences in peak shapes due to kinetic energy released or required in the various fragmentation processes [50–52].

All calculations were performed using the GAUSSIAN 03 suite of programs [53]. Structural parameters of $C_3H_5O^{-/0/+}$ species and their fragments were optimized at the B3LYP/6−311+G(2d,p) level of theory [54–57]. Stationary points were characterized as minima (no imaginary frequencies) or as transition structures (one imaginary frequency) using vibrational frequency calculations at the same level of theory. More accurate energies of the optimized structures were obtained from the single-point calculations performed at the CCSD(T)/6−311+G(3df,3pd) level of theory [58–61]. Energies given below refer to 0 K and are derived from the electronic energies of the CCSD(T) calculations corrected for the zero-point vibrational energies obtained at the B3LYP level.

3. Results and discussion

3.1. Neutralization–reionization mass spectrum of $CH_2=CHCH_2O^-$

As a precursor for the generation of the neutral allyloxy radical, we used the $C_3H_5O^-$ anion generated in good yields by deprotonation of allyl alcohol in the negative-ion chemical ionization mode. The electron affinity of the allyloxy radical amounts to $EA(CH_2=CHCH_2O^\bullet)=(2.01\pm0.03)$ eV and (1.95 ± 0.03) eV for the cisoid and gauche rotamers, respectively.[1] Hence, electron detachment should be relatively facile compared to other fragmentations occurring at the anionic stage [62]. In contrast, vertical ionization of the neutral species to the cationic counterparts generally is rather unfavorable for alkoxy radicals because the resulting RO^+ ions are electron-deficient species which only exist in the triplet state, whereas the singlet electromers spontaneously isomerize and then rapidly dissociate due to their large internal energy content, e.g.: $CH_3O^\bullet \rightarrow {}^1CH_3O^{+\bullet} \rightarrow {}^1CH_2OH^{+\bullet} \rightarrow {}^1HCO^+ + H_2$ [34,36]. As a consequence, the $^-CR^+$ and $^-NR^+$ spectra of alkoxide ions never exhibit large, and often do not show any, significant survivor ion signals [35,37,49,63,64].

Fig. 2 shows the $^-CR^+$ and $^-NR^+$ spectra of mass-selected $C_3H_5O^-$ anions generated by deprotonation of allyl alcohol. Both spectra have an overall similar appearance and are characterized by a large amount of fragmentation to the $(C_2H_n + CH_mO)^+$ manifold (m/z 24–31) as compared to the $C_3H_nO^+$ species in the range from m/z 52 to 58. Nevertheless, several notable differences are observed which are best highlighted in the neutral-and-ion decomposition difference (NIDD) spectrum as shown in Fig. 2c. For obtaining the $^-NIDD^+$ spectrum, the $^-CR^+$ is subtracted from the $^-NR^+$ spectrum after normalization such that the negative signals indicate processes which preferentially occur at the ionic stage, whereas the positive signals are due to reactions of the neutral intermediates formed in the $^-NR^+$ sequence.

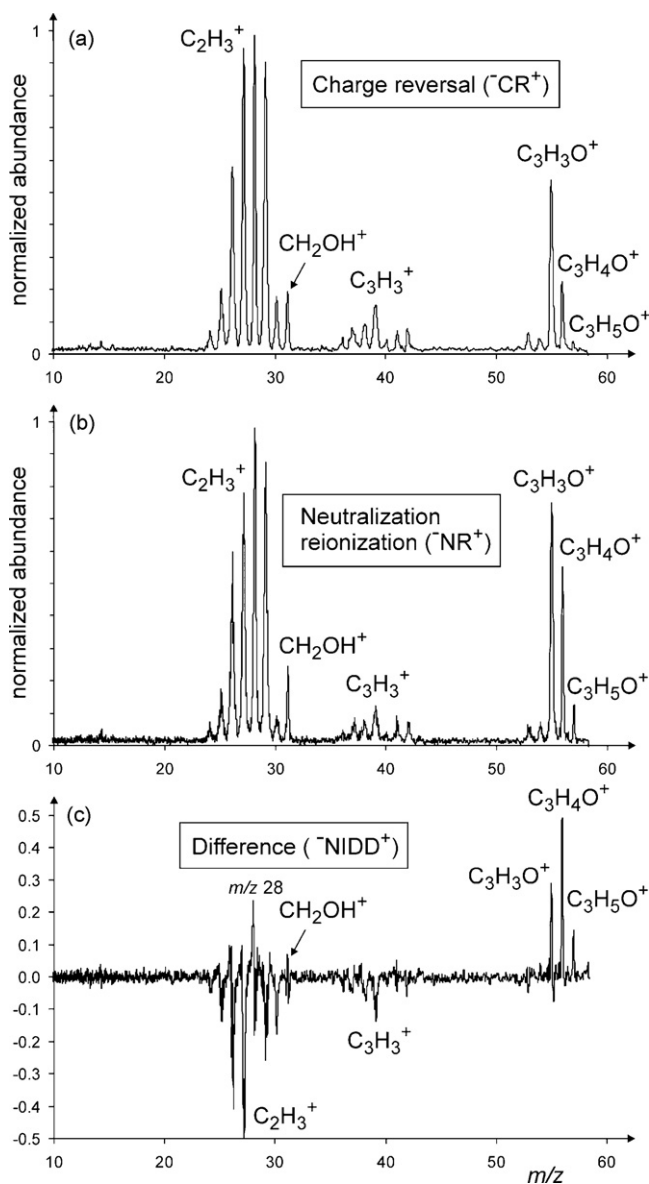[1] R.E. Continetti, La Jolla, USA, private communication.

Fig. 2. (a) Charge reversal, (b) neutralization–reionization, and (c) the derived NIDD spectrum of mass-selected $CH_2=CHCH_2O^-$ generated by negative ion chemical ionization of allyl alcohol using N_2O as reagent gas (collision gases O_2/O_2 with 80% transmission each).

Upon inspection of Fig. 2c it becomes obvious that the entire mass region of the $C_3H_nO^+$ signals in which the heavy atom skeleton remained intact is associated with positive $^-NIDD^+$ signals. Such a result can indicate either (i) that the geometries of the anionic and cationic states differ significantly and that the neutral species, having an intermediate geometry can act as a mediator or (ii) that the species formed via vertical neutralization of the ionic precursor easily undergo dissociation to C_3H_nO ($n < 6$) fragments which accordingly gives rise to a positive $^-NIDD^+$ signal. Another intriguing aspect concerns the similarity of the $^-CR^+$ and $^-NR^+$ spectra in the region of the $C_3H_nO^+$ ions with the photoionization mass spectra of the neutral C_3H_nO product reported by Siebert and coworkers (Fig. 1a). Thus, the abundance of the signal at m/z 57 is small in Fig. 2a and b compared to m/z 55 and 56 of which the former, representing the closed-shell species $C_2H_3CO^+$, gives rise to the base peak in this mass range. A rather similar pattern is observed in Fig. 1a, where in addition to "C_3H_6O" species from reaction (1), also "C_3H_4O" could contribute to some extent (reaction (1a)). Among the

Table 1
Calculated energetics (in eV) of the $C_3H_5O^{-/0/+}$ species at the B3LYP/6−311+G(2d,p) and CCSD(T)/6−311+G(3df,3pd)//B3LYP/6−311+G(2d,p) level of theory. All energetics are given relative to the allyloxide ion which is the energetically most stable species and serves as a precursor in the mass spectrometric experiments. E_{rel}^{el} refers to the potential energies at equilibrium energy, while E_{rel}^{0K} includes the zero-point energy.

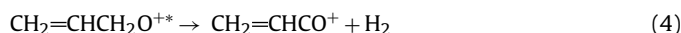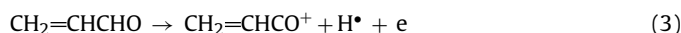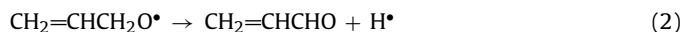|	State	B3LYP	CCSD(T)//B3LYP			
		E_{rel}^{0K}	E_{rel}^{0K}	E_{rel}^{el}	E_v (anion)[a]	E_v (neutral)[b]
$CH_2CHCH_2O^-$ (cisoid)	$^1A'$	0.00	0.00	0.00		
$CH_2CHCH_2O^•$ (cisoid)	$^2A''$	1.88	1.84	1.82	2.01	
$CH_2CHCH_2O^•$ (cisoid)	$^2A'$	2.28	2.20	1.91	2.12	
$CH_2CHCH_2O^+$	$^1A'$	_[c]	_[c]	_[c]	12.05	9.97[d]
$CH_2CHCH_2O^+$	^3A	11.51	11.74	11.73	12.09	10.28
$CH_2CHCH_2O^-$ (gauche)	^1A	0.08	0.07	0.06		
$CH_2CHCH_2O^•$ (gauche)	^2A	1.90	1.86	1.81	1.92	
$CH_2CHCHOH^-$ (cisoid)	^1A	0.51	0.48	0.48		
$CH_2CHCHOH^•$ (cisoid)	$^2A''$	0.89	0.82	0.74	0.50	
$CH_2CHCHOH^+$ (cisoid)	$^1A'$	8.01	7.84	7.68	8.38	7.14
$CH_2CHCHOH^-$ (transoid)	^1A	0.74	0.75	0.77		
$CH_2CHCHOH^•$ (transoid)	$^2A''$	0.90	0.85	0.79	0.44	
$CH_2CHCHOH^+$ (transoid)	$^1A'$	7.89	7.73	7.56	8.54	7.03

[a] Vertical transition from the anion; energy refers to the difference of electronic energies.
[b] Vertical transition from the neutral; energy refers to the difference of electronic energies.
[c] The vertical ionization energy to the excited $^2A'$ state amounts to 2.12 eV.
[d] VIE from the $^2A''$ state of the radical.

differences between the $^-CR^+$ and $^-NR^+$ spectra a significant feature concerns the ratio of the signals for $CH_2O^{•+}$ and CH_2OH^+ (m/z 30 and 31) which changes from ca. 1:1 in $^-CR^+$ to ca. 1:3 in $^-NR^+$. Further, we note that several peaks in the $^-NIDD^+$ spectrum show an oscillating behavior due to different peak broadening in the $^-CR^+$ and $^-NR^+$ experiments [42], e.g., the peak at m/z 28 in Fig. 2c. While we do not dwell upon these differences in the present context of reaction (1), these peak broadenings reflect the kinetic energy releases associated with the dissociations in the various charge states and thus have mechanistic significance which is not recognized if only nominal masses are considered in NIDD spectra.

$$CH_2=CHCH_2O^• \rightarrow CH_2=CHCHO + H^• \quad (2)$$

$$CH_2=CHCHO \rightarrow CH_2=CHCO^+ + H^• + e \quad (3)$$

$$CH_2=CHCH_2O^{+*} \rightarrow CH_2=CHCO^+ + H_2 \quad (4)$$

In previous $^-CR^+$ and $^-NR^+$ studies of saturated alkoxide ions [34–37,49], the major fragmentations observed were assigned to α-cleavages of the neutral alkoxy radicals and to 1,1-dehydrogenation upon reionization. By analogy, we qualitatively attribute the abundant signals at m/z 55 and 56 in Fig. 2a and b to the loss of atomic hydrogen to afford acrolein at the neutral stage (reaction (2)), dissociative ionization of acrolein in the reionization step (reaction (3)), and dehydrogenation of the transient allyloxy cation at the cation stage (reaction (4)). Likewise, the positive $^-NIDD^+$ signals for $C_3H_5O^+$ and $C_3H_4O^+$ can be explained by reference to the previous studies of gaseous alkoxide ions. Thus, rearrangement of transient $CH_2=CHCH_2O^•$ to an oxiranylmethyl radical [15,16] converts an oxygen- to a carbon-centered radical (Scheme 1) which is more likely to yield an intact $C_3H_5O^+$ cation in the subsequent reionization step, and the increased yield of $C_3H_4O^{•+}$ is a direct consequence of the occurrence of reaction (2). According to theoretical studies of Smith et al., the barrier associated with the ring closure amounts to only 0.23 eV [65]. The less abundant but also positive $^-NIDD^+$ signal due to $C_3H_3O^+$ can accordingly be interpreted as a consequence of the occurrence of reactions (2)–(4).
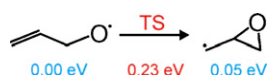
Scheme 1. Ring-closure of allyloxy radical to the oxiranylmethyl radical (energetics taken from Ref. [65]).

3.2. Potential energy surface relevant in the collisional electron transfer

In order to probe the above arguments and shed further light on the energetics of the electron transfer processes involved, the relevant parts of the potential energy surfaces of the $C_3H_5O^{-/0/+}$ system have been studied by quantum chemistry. Table 1 gives the energies of fully optimized geometries of the relevant species at the B3LYP level of theory as well as single-point energy calculated at the CCSD(T) level at the B3LYP geometries. The hybrid density functional and the wavefunction-based ab initio methods agree with maximal deviations of about ±0.2 eV for the cation states, which is sufficiently good for the considerations made here.

The allyloxide anion has a cisoid geometry with a vertical detachment energy of $DE_v = 2.01$ eV, while the adiabatic electron affinity of the allyloxy radical is calculated as $EA_a = 1.84$ eV. The gauche conformation of the anion is only slightly higher in energy and has a similar EA. These values are in reasonable agreement with a preliminary experimental $EA(CH_2=CHCH_2O^•)$ of (2.01 ± 0.03) eV, kindly communicated by Continetti (see footnote 1). While the energy deposited in the neutral radical upon vertical electron detachment is somewhat lower than the lowest-lying dissociation channel to afford acrolein and $H^•$ (0.52 eV, Fig. 3), the low energy threshold for H atom loss is consistent with the assumed occurrence of reaction (2) in the $^-NR^+$ experiment and thus the positive $^-NIDD^+$ signal for $C_3H_4O^+$. As expected by analogy to the methoxy cation [34–36], the allyloxy cation is a minimum only on the triplet surface, whereas the singlet does not correspond to a stationary point and loss of molecular hydrogen via 1,1-dehydrogenation is highly exothermic (Fig. 3). Accordingly, the survivor ion for $C_3H_5O^+$ in the $^-CR^+$ experiment is small (Fig. 2a). As outlined above, the increased relative abundance of the survivor ion in the $^-NR^+$ spectrum (Fig. 2b) and thus the positive $^-NIDD^+$ signal for $C_3H_5O^+$ can be attributed to the previously described rearrangement of the neutral radical into the oxiranylmethyl radical [15,16], whose barrier of only 0.23 eV [65] is lower than the energy required for H-atom loss according to reaction (2); thus, the occurrence of this rearrangement appears quite feasible.

As a conceivable alternative, we probed the rearrangement of the allyloxy radical into the hydroxyallyl radical, which is considerably more stable than the former ($\Delta E_{rel} = 1.03$ eV) due to the change from an oxygen-centered to a carbon-centered radical concomitant with the conjugation in allyl system (Fig. 4). Such a rearrangement promoted by alcohols has been observed in the condensed
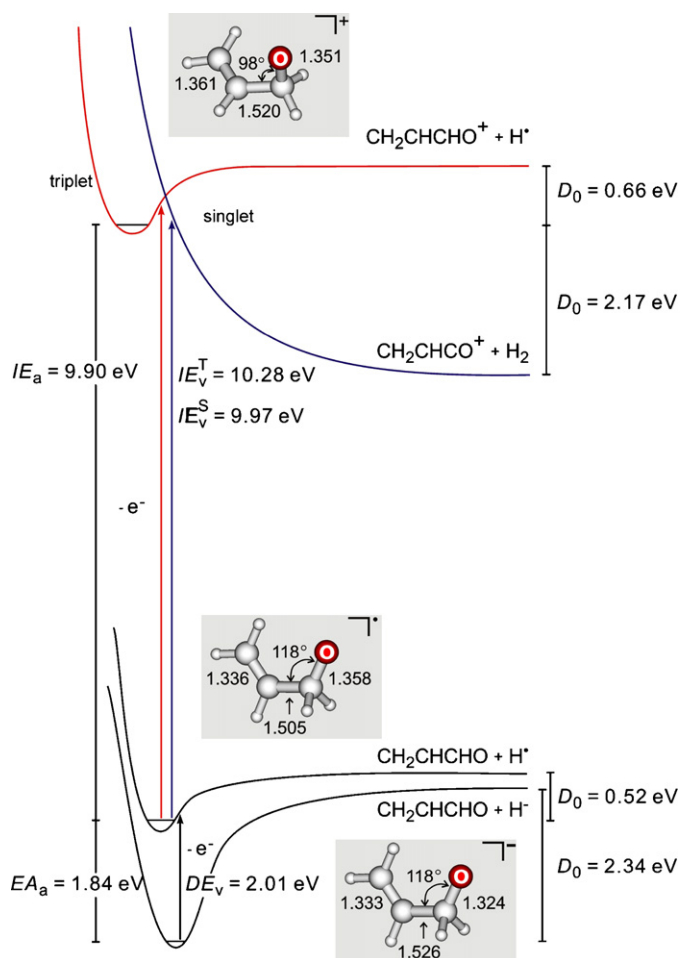
Fig. 3. Schematic potential-energy surface (CCSD(T)/6−311+G(3df,3pd)//B3LYP/6−311+G(2d,p)) for the transition of the CH_2=$CHCH_2O^-$ anion to the neutral alkoxy radical and the subsequent reionization to the cationic species. The minimum for the cation corresponds to the triplet state (red color), while the singlet state of the cation leads to the elimination of H_2 (blue color).
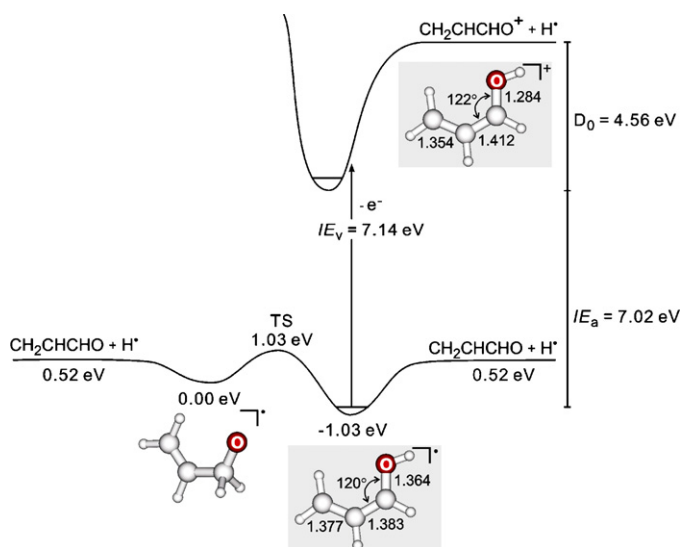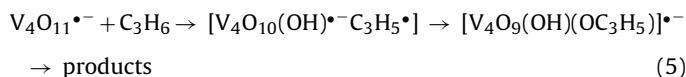

Fig. 4. Potential-energy surface (CCSD(T)/6−311+G(3df,3pd)//B3LYP/6−311+G(2d,p)) for the rearrangement of the allyloxy radical to the hydroxyallyl radical and subsequent ionization to the manifold of protonated acrolein. Relative energies are given at 0 K.

phase by means of EPR spectroscopy [17]. While the energy barrier associated with the required H-atom shift is relatively low (1.02 eV relative to allyloxy), it is located 0.50 eV above the energy demand for H-atom loss and thus reaction (2) is likely to predominate over this particular isomerization channel. Nevertheless, the rearrangement depicted in Fig. 4 may to some extent contribute to the positive $^-NIDD^+$ signal for $C_3H_5O^+$ in Fig. 2c, whose major share is however attributed to the rearrangement to the oxiranylmethyl radical as described above. In addition, we briefly investigated the occurrence of a similar rearrangement already at the anionic stage. However, the corresponding hydroxyallyl anion is 0.48 eV less stable than the allyloxide tautomer CH_2=CH–CH_2–O^-, and the former is thus less likely to contribute to the beam of mass-selected $C_3H_5O^-$ ions formed upon chemical ionization in the presence of an excess of allyl alcohol. The energy barrier for the rearrangement of the allyloxide anion to the hydroxyallyl anion amounts to 1.98 eV, thus it is below the dissociation limit for the hydride elimination. In agreement, Continetti reports evidence for this isomer when $C_3H_5O^-$ is formed by H abstraction with $O^{-\bullet}$ in a pulsed discharge expansion (see footnote 1).

4. Conclusions

Neutralization–reionization and charge-reversal studies of the allyloxide anion provide insight into the unimolecular reactions of the transient allyloxy radical formed upon electron detachment from the anion precursor. Inter alia these results also suggest allyloxy units as a possible candidate to explain the photoionization patterns recently reported by Siebert and coworkers in their experimental probe of the oxygenate formed in the reaction of the vanadium-oxide cluster $V_4O_{11}{}^{\bullet-}$ with propene [20]. Consequently, we propose that the initial step of reaction (1) involve an allylic C–H bond activation of propene concomitant with hydrogen-atom transfer to the cluster, followed by recombination of the allyl radical with another oxo ligand of the cluster to afford an allyloxy unit bound to the cluster ion (reaction (5)). In the photodetachment/photoionization experiment, the latter unit could then be liberated and ionized into cationic species, whose pattern reported in Ref. [20] is quite comparable to those in Fig. 2a and b.

$$V_4O_{11}{}^{\bullet-} + C_3H_6 \rightarrow [V_4O_{10}(OH)^{\bullet-}C_3H_5{}^\bullet] \rightarrow [V_4O_9(OH)(OC_3H_5)]^{\bullet-}$$

$$\rightarrow \text{products} \tag{5}$$

If this scenario holds true, an important consequence is that the high-valent vanadium-oxide anion does not enable the epoxidation of propene to propylene oxide, but instead mediates allylic hydroxylation via initial H-atom abstraction [33,66].

Acknowledgements

References

[1] M.J. Pilling, Ann. Rev. Phys. Chem. 47 (1996) 81.
[2] N. Balucani, Int. J. Mol. Sci. 10 (2009) 2304.
[3] J.-H. Choi, Int. Rev. Phys. Chem. 25 (2006) 613.
[4] P. Casavecchia, F. Leonori, N. Balucani, R. Petrucci, G. Capozza, E. Segoloni, Phys. Chem. Chem. Phys. 11 (2009) 46.
[5] M. Sablier, C. Rolando, Mass Spectrom. Rev. 12 (1993) 285.
[6] X. Zhang, S. Kato, V.M. Bierbaum, M.R. Nimlos, G.B. Ellison, J. Phys. Chem. A 108 (2004) 9733.

[7] A.L. Russell, H.W. Rohrs, D. Read, D.E. Giblin, P.P. Gaspar, M.L. Gross, Int. J. Mass Spectrom. 287 (2009) 8.
[8] H.C. Kwon, J.H. Park, H. Lee, H.K. Kim, Y.S. Choi, J.H. Choi, J. Chem. Phys. 116 (2002) 2575.
[9] J.H. Park, H. Lee, H.C. Kwon, H.K. Kim, Y.S. Choi, J.H. Choi, J. Chem. Phys. 117 (2002) 2017.
[10] J.H. Park, H. Lee, J.H. Choi, J. Chem. Phys. 119 (2003) 8966.
[11] S.K. Joo, L.K. Kwon, H. Lee, J.H. Choi, J. Chem. Phys. 120 (2004) 7976.
[12] F. Leonori, N. Balucani, G. Capozza, E. Segoloni, D. Stranges, P. Casavecchia, Phys. Chem. Chem. Phys. 9 (2007) 1307.
[13] B.L. FitzPatrick, K.-C. Lau, L.J. Butler, A.-H. Lee, J.J.-M. Lin, J. Chem. Phys. 129 (2008) 084301.
[14] K. Hoyermann, F. Nacke, J. Nothdurft, M. Olzmann, J. Wehmeyer, T. Zeuch, Proc. Combust. Inst. 32 (2009) 157.
[15] D.J. Pasto, F. Cottard, C. Picconatto, J. Org. Chem. 59 (1994) 7122.
[16] F.E. Ziegler, A.K. Petersen, J. Org. Chem. 60 (1995) 2666.
[17] P.E. Elford, B.P. Roberts, J. Chem. Soc. Perkin Trans. 2 (1996) 2247.
[18] A.L. Cooks, H.F. King, W.H. Richardson, J. Org. Chem. 68 (2003) 9441.
[19] L.S. Alconcel, H.J. Deyerl, M. DeClue, R.E. Continetti, J. Am. Chem. Soc. 123 (2001) 3125.
[20] S. Li, A. Mirabal, J. Demuth, L. Wöste, T. Siebert, J. Am. Chem. Soc. 130 (2008) 16832.
[21] S. Feyel, D. Schröder, H. Schwarz, J. Phys. Chem. A 110 (2006) 2647.
[22] S. Feyel, D. Schröder, X. Rozanska, J. Sauer, H. Schwarz, Angew. Chem. Int. Ed. 45 (2006) 4677.
[23] D. Schröder, D. Sülzle, J. Hrušák, D.K. Böhme, H. Schwarz, Int. J. Mass Spectrom. Ion Processes 110 (1991) 145.
[24] D. Schröder, H. Schwarz, Helv. Chim. Acta 75 (1992) 1281.
[25] D. Schröder, J. Müller, H. Schwarz, Organometallics 12 (1993) 1972.
[26] D. Schröder, H. Schwarz, S. Polarz, M. Driess, Phys. Chem. Chem. Phys. 7 (2005) 1049.
[27] C. Wesdemiotis, F.W. McLafferty, Chem. Rev. 87 (1987) 485.
[28] J.K. Terlow, H. Schwarz, Angew. Chem. Int. Ed. Engl. 26 (1987) 865.
[29] N. Goldberg, H. Schwarz, Acc. Chem. Res. 27 (1994) 347.
[30] F. Tureček, Top. Curr. Chem. 225 (2003) 77.
[31] J. Schwarz, R. Wesendrup, D. Schröder, H. Schwarz, Chem. Ber. 129 (1996) 1463.
[32] J. Roithová, D. Schröder, J. Am. Chem. Soc. 129 (2007) 15311.
[33] J. Roithová, D. Schröder, Chem. Rev. 110 (2010) 1170.
[34] P.C. Burgers, J.L. Holmes, Org. Mass Spectrom. 19 (1984) 452.
[35] R.S. Mercer, A.G. Harrison, Org. Mass Spectrom. 22 (1987) 710.
[36] M. Aschi, J.N. Harvey, C.A. Schalley, D. Schröder, H. Schwarz, J. Chem. Soc. Chem. Commun. (1998) 531.
[37] G. Hornung, C.A. Schalley, M. Dieterle, D. Schröder, H. Schwarz, Chem. Eur. J. 3 (1997) 1866.
[38] M.J. Polce, C. Wesdemiotis, J. Am. Soc. Mass Spectrom. 7 (1996) 573.
[39] M.J. Polce, C. Wesdemiotis, J. Am. Soc. Mass Spectrom. 6 (1995) 1030.
[40] M. Gu, F. Tureček, Org. Mass Spectrom. 29 (1994) 94.
[41] H.C.M. Byrd, L.M. Castro, Y.-Q. Yu, T. Hwang, H.I. Kenttämaa, Int. J. Mass Spectrom. Ion Processes 167/168 (1997) 403.

[42] C.A. Schalley, D. Schröder, H. Schwarz, Int. J. Mass Spectrom. Ion Processes 153 (1996) 173.
[43] H. Schwarz, Pure Appl. Chem. 61 (1989) 685.
[44] M.M. Bursey, Mass Spectrom. Rev. 9 (1990) 555.
[45] A.S. Danell, G.L. Glish, Int. J. Mass Spectrom. 212 (2001) 219.
[46] J.H. Bowie, Int. J. Mass Spectrom. 212 (2001) 249.
[47] A.W. McMahon, S.K. Chowdhury, A.G. Harrison, Org. Mass Spectrom. 24 (1989) 620.
[48] C.A. Schalley, G. Hornung, D. Schröder, H. Schwarz, Int. J. Mass Spectrom. 172/173 (1998) 181.
[49] C.A. Schalley, G. Hornung, D. Schröder, H. Schwarz, Chem. Soc. Rev. 27 (1998) 91.
[50] D. Schröder, in: P.B. Armentrout (Ed.), Encyclopedia of Mass Spectrometry, vol. 1, Elsevier, Amsterdam, 2003, p. 521.
[51] D. Schröder, R. Brown, P. Schwerdtfeger, X.-B. Wang, X. Yang, L.-S. Wang, H. Schwarz, Angew. Chem. Int. Ed. 42 (2003) 311.
[52] J. Roithová, D. Schröder, H. Schwarz, Angew. Chem. Int. Ed. 44 (2005) 3092.
[53] M.J. Frisch, G.W. Trucks, H.B. Schlegel, G.E. Scuseria, M.A. Robb, J.R. Cheeseman, J. Montgomery, T. Vreven, K.N.B. Kudin, J.M. Millam, S.S. Iyengar, J. Tomasi, V. Barone, B. Mennucci, M. Cossi, G. Scalmani, N. Rega, G.A. Petersson, H. Nakatsuji, M. Hada, M. Ehara, K. Toyota, R. Fukuda, J. Hasegawa, M. Ishida, T. Nakajima, Y. Honda, O. Kitao, H. Nakai, M. Klene, X. Li, J.E. Knox, H.P. Hratchian, J.B. Cross, V. Bakken, C. Adamo, J. Jaramillo, R. Gomperts, R.E. Stratmann, O. Yazyev, A.J. Austin, R. Cammi, C. Pomelli, J.W. Ochterski, P.Y. Ayala, K. Morokuma, G.A. Voth, P. Salvador, J.J. Dannenberg, V.G. Zakrzewski, S. Dapprich, A.D. Daniels, M.C. Strain, O. Farkas, D.K. Malick, A.D. Rabuck, K. Raghavachari, J.B. Foresman, J.V. Ortiz, Q. Cui, A.G. Baboul, S. Clifford, J. Cioslowski, B.B. Stefanov, G. Liu, A. Liashenko, P. Piskorz, I. Komaromi, R.L. Martin, D.J. Fox, T. Keith, M.A. Al-Laham, C.Y. Peng, A. Nanayakkara, M. Challacombe, P.M.W. Gill, B. Johnson, W. Chen, M.W. Wong, C. Gonzalez, J.A. Pople, GAUSSIAN 03, Revision C.02, 2004.
[54] S.H. Vosko, L. Wilk, M. Nusair, Can. J. Phys. 58 (1980) 1200.
[55] C. Lee, W. Yang, R.G. Parr, Phys. Rev. B 37 (1988) 785.
[56] A.D. Becke, Phys. Rev. A 38 (1988) 3098.
[57] B. Miehlich, A. Savin, H. Stoll, H. Preuss, Chem. Phys. Lett. 157 (1989) 200.
[58] J. Cizek, Adv. Chem. Phys. 14 (1969) 35.
[59] G.D. Purvis, R.J. Bartlett, J. Chem. Phys. 76 (1982) 1910.
[60] G.E. Scuseria, C.L. Janssen, H.F. Schaefer III, J. Chem. Phys. 89 (1988) 7382.
[61] J.A. Pople, M. Head-Gordon, K. Raghavachari, J. Chem. Phys. 87 (1987) 5968.
[62] S. Dua, J.H. Bowie, R.N. Hayes, Rapid Commun. Mass Spectrom. 7 (1993) 336.
[63] U. Dreyer, D. Sülzle, D. Schröder, H. Schwarz, Helv. Chim. Acta 73 (1990) 2179.
[64] S. Kostka, D. Schröder, D. Sülzle, H. Schwarz, Int. J. Mass Spectrom. Ion Processes 117 (1992) 15.
[65] D.M. Smith, A. Nicolaides, B.T. Golding, L. Radom, J. Am. Chem. Soc. 120 (1998) 10223.
[66] S. Feyel, J. Döbler, R. Höckendorf, M.K. Beyer, J. Sauer, H. Schwarz, Angew. Chem. Int. Ed. 47 (2008) 1946.